Advanced Math. Models & Applications
Vol.2, No.2, 2017, pp.117-138

PENNY SHAPED CRACK IN AN INFINITE TRANSVERSELY ISOTROPIC PIEZOELECTRIC LAYER UNDER SYMMETRICALLY APPLIED LINE LOAD

Rajesh Patra[1], Sakti Pada Barik[2], P.K.Chaudhuri[3]

[1]Department of Mathematics, Hooghly Engineering & Technology College, Vivekananda Road, Hooghly-712103, India
[2]Department of Mathematics, Gobardanga Hindu College, 24-Parganas (N), Pin-743273, India
[3] Retired Professor, Department of Applied Mathematics, University of Calcutta, 92, A.P.C. Road,Kolkata-700009, India

Abstract. The present paper is concerned with the study of an internal penny shaped crack problem in an infinite transversely isotropic piezoelectric layer. The crack is supposed to be opened by an internal uniform pressure p_0 along its faces. The layer surfaces are assumed to be acted upon by a uniformly applied line load of magnitude P acting along the circumference of a circle of radius $a(<b)$ .The applied load may be tensile or compressive in nature. Furthermore, it is assumed that the line joining the centers of the two line load circles passes through the center of the penny shaped crack and is perpendicular to the plane of the crack. Due to the assumed symmetries in material properties as well as the symmetry in applied loadings the present problem can easily be modeled as a two dimensional problem. Using Hankel transform technique the solution of the problem has been reduced to the solution of two singular integral equations. The integral equations are solved numerically. The stress-intensity factor and the crack opening displacements are determined and the effects of piezoelectricity and anisotropy on them in both the cases are shown graphically.

Keywords: *piezoelectric medium, transversely isotropic medium, integral transform, Fredholm integral equation, stress-intensity factor.*

AMS Subject Classification: *97M10.*

Corresponding Author: *Dr. Sakti Pada Barik, Department of Mathematics, Gobardanga Hindu College,24-Parganas (N),Pin-743273, India, e-mail: spbarik1@gmail.com*

Manuscript received: *12 February2017*

1. Introduction

In course of the study of various properties of solid materials, the discovery of the piezoelectric effect has attracted the special attention of the scientists. Piezoelectric effect was discovered by Jacques and Pierre Curie in 1880. It was found that during deformation of some crystals there was generation of electric charges on their surfaces. The reverse effect was observed in 1881 in which application of electric field on the boundary of certain crystals generates stress and strain in those crystals. These materials turn out to be very useful for their very special and unusual properties to produce electrical energy through use of mechanical loadings. Piezoelectric

materials, in particular, piezoelectric ceramics, have been widely used for applications in various fields such as sensors, filters, ultrasonic generators, actuators, laser, supersonics, microwave, navigation and biology. Piezoelectric composite materials are also in use in hydrophone application and transducers for medical imaging. Considering the huge applicability of these materials in various fields, solid mechanics problems are being studied in solids with piezoelectric properties.

The determination of the state of stress in medium under applied load has been the subject of study in literature for many years. The study needs special attention and care when the elastic body develops a crack in it. Presence of a crack in a structure not only affects the stress distribution in it but also drastically reduces the life span of the structure. Presence of a crack in a solid also significantly changes its response to the applied load. Stress distributions in the solid with a crack are studied in two regions: the region in the neighborhood of crack, called the near field region and the region far away from the crack, called the far field region. Study of stress distribution in the near field region is very important because of the generation of stress of very high magnitude at the crack boundary leading to possible spread of crack. Stress intensity factor, crack energy etc. are some of the measurable quantities used for checking possible crack expansion. For a solid with a crack in it loaded mechanically or thermally [2, 4, 5, 8, 10, 11, 12, 17, 18] determination of stress intensity factor (SIF) becomes a very important task in fracture mechanics. SIF needs to be understood if we are to design fracture tolerant materials used in bridges, buildings, aircraft, or even bells. Polishing just won't do if we detect crack. Crack problems in piezoelectric medium have been studied in literature following classical theory. A comprehensive list of work on crack problems in piezoelectric media done by earlier investigators can be found in [1, 3, 6, 7, 13, 16, 19, 20, 21, 23, 24].

The present investigation aims at investigating an internal penny shaped crack problem in an infinite transversely isotropic piezoelectric layer. The crack faces are parallel to the layer surfaces and the layer surfaces are under the action of compressive or tensile line loads applied along the circumference of circle such that the line joining the centers of these circles is perpendicular to the plane of the crack and passing to its centre. Hankel transform of different orders are applied on the governing equations and boundary conditions. Thereafter, using operator theory a general solution in terms of three potential functions has been derived. These functions satisfy differential equations of the second order and are quasi-harmonic functions. Making use of these fundamental solutions, the crack problem in the aforesaid case is investigated. The solution of the problem has been reduced to the solution of Fredholm type integral equation of second kind which requires numerical treatment. Numerical solution is obtained through the process of discretization of the integrals, and based on the available parameter values, evaluation of stresses, SIF etc are obtained. Finally, a discussion is made on the obtained results presented graphically.

2. Formulation of the problem

We consider an infinite elastic layer of thickness 2h weakened by an internal penny shaped crack of radius b lying in the middle of the layer and opened by a pressure p_0 on its faces (Fig.1). The material of the layer is elastically transversely isotropic with piezoelectric properties. The layer surfaces are subjected to circular line loads symmetrically applied with respect to the center of the penny shaped crack. Let $a(< b)$ be the radius of the circle on which a load P is uniformly distributed, so that the load per unit length is $\frac{P}{2\pi a}$. The applied load may be tensile or compressive in nature acting perpendicularly to the layer surfaces. We shall use cylindrical coordinate system (r,θ,z) with origin at the centre of the crack and z-axis along the normal to the free surface.

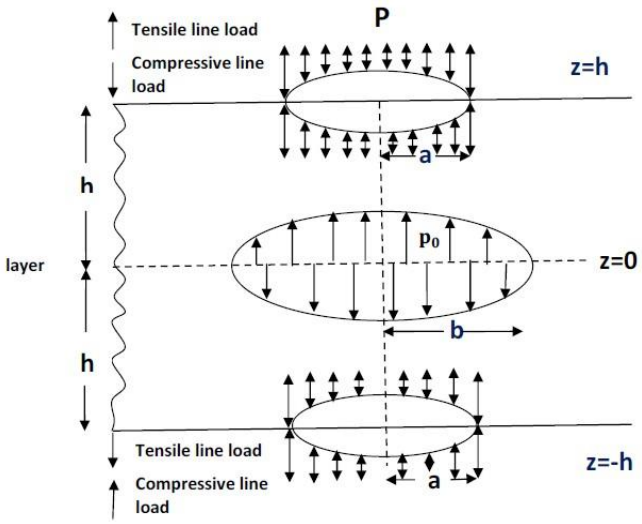

Fig.1. Geometry of the problem

We shall also make the following additional assumptions:

(i) There is no force of gravity
(ii) The axis of symmetry of the transversely isotropic material is along the z- axis
(iii) The axis of polarization of the piezoelectric material coincides with the z - axis
(iv) Strains and displacements are small so as to apply linear theory

Because of assumed axisymmetry in elastic and piezoelectric properties and the nature of the applied load, the displacement vector $\vec{u} = (u_r, u_\theta, u_z)$ will have its cross radial component $u_\theta = 0$ and all the physical quantities are

independent of θ. The problem may thus be considered as a two dimensional one in the $r-z$ plane with $0 \le r < \infty$ and $-h \le z \le h$.

The mathematical formulation of the problem consists of

(A) ***Equilibrium equations:***

$$\left.\begin{aligned} C_{11}\pounds_1 u_r + C_{44}D^2 u_r + (C_{13} + C_{44})\mathrm{D}\frac{\partial u_z}{\partial r} + (e_{31} + e_{15})D\frac{\partial \phi}{\partial r} = 0, \\ C_{44}\pounds_0 u_z + C_{33}D^2 u_z + (C_{13} + C_{44})\mathrm{D}\frac{\partial [r u_r]}{r\partial r} + e_{15}\pounds_0 \phi + e_{33}D^2\phi = 0, \\ (e_{31} + e_{15})D\frac{\partial [r u_r]}{r\partial r} + e_{15}\pounds_0 u_z + e_{33}D^2 u_z - \epsilon_{11}\pounds_0 \phi - \epsilon_{33}D^2\phi = 0. \end{aligned}\right\} \quad (1)$$

where

$$\pounds_k = \frac{\partial^2}{\partial r^2} + \frac{1}{r}\frac{\partial}{\partial r} - \frac{k}{r^2}; \qquad k = 0,1, \quad D = \frac{\partial}{\partial z},$$

and

(B) ***The boundary conditions:***

$$\frac{\partial}{\partial r}[u_z(r,0)] = \begin{cases} f(r), & 0 \le r < b; \\ 0, & b < r < \infty, \end{cases} \quad (2)$$

$$\sigma_{rz}(r,0) = 0, (0 \le r < \infty), \quad (3)$$

$$\sigma_{zz}(r,h) = \mp\frac{P}{2\pi a}\delta(r-a), \quad (0 \le r < \infty), \quad (4)$$

$$\sigma_{zz}(r,0) = -p_0, (0 \le r \le b), \quad (5)$$

$$\sigma_{rz}(r,h) = 0, (0 \le r < \infty), \quad (6)$$

$$D_z(r,0) = 0, (|r| > b), \quad (7)$$

$$\Phi(r,0) = 0, (0 \le r \le b), \quad (8)$$

$$\Phi(r,h) = \Phi_0, (r \ge 0), \quad (9)$$

$$\frac{\partial \phi(r,0)}{\partial r} = 0, \quad (|r| > b). \quad (10)$$

The parameters C_{ij} appearing in (1) are the elastic coefficients whereas e_{kl} and ϵ_{kl} are piezoelectric and dielectric constants respectively of the material. In addition to the boundary conditions, the displacement components and the potential function ϕ should satisfy the regularity condition $u_r, u_z, \phi \to 0$ as $\sqrt{r^2 + z^2} \to \infty$. Here $f(r)$ is an unknown function and $\delta(r)$ is the Dirac delta function. In equation (4) positive sign indicates tensile force while negative sign corresponds to compressive force.

2. Method of solution

Solution of the partial differential equations (1) requires application of Hankel transform of different order. We shall follow the method adopted by [7] in our solution process. For clarity in our method of solution it would be better if briefly outline the first part of the method adopted by [7] here. We shall use Hankel transform with respect to variable r to be denoted by $\hat{}$, of

the functions u_r, u_z, Φ such that

$$\widehat{u_r}(\xi,z)=\int_0^\infty u_r(r,z)rJ_1(r\xi)dr, \tag{11}$$

$$\{\widehat{u_z}(\xi,z),\hat{\phi}(\xi,z)\}=\int_0^\infty \{u_z(r,z),\Phi(r,z)\}rJ_0(r\xi)dr \tag{12}$$

where J_0 and J_1 are the Bessel functions of the first kind and of order zero or one, respectively, and ξ is the transform parameter.

Using properties of Hankel transformation we obtain

$$A\begin{bmatrix}\widehat{u_r}\\ \widehat{u_z}\\ \hat{\phi}\end{bmatrix}=\begin{bmatrix}0\\0\\0\end{bmatrix}, \tag{13}$$

where

$$A=\begin{bmatrix}-C_{11}\xi^2+C_{44}D^2 & -\xi(C_{13}+C_{44})D & -\xi(e_{31}+e_{15})D\\ \xi(C_{13}+C_{44})D & -C_{44}\xi^2+C_{33}D^2 & -e_{15}\xi^2+e_{33}D^2\\ \xi(e_{31}+e_{15})D & -e_{15}\xi^2+e_{33}D^2 & \epsilon_{11}\xi^2-\epsilon_{33}D^2\end{bmatrix}. \tag{14}$$

It can be easily found that

$$|A|=-a_0(D^2-\lambda_1^2\xi^2)(D^2-\lambda_2^2\xi^2)(D^2-\lambda_3^2\xi^2), \tag{15}$$

where $\lambda_i^2(i=1,2,3)$ are the roots of the following cubic algebraic equation

$$a_0\lambda^6+b_0\lambda^4+c_0\lambda^2+d_0=0 \tag{16}$$

with the coefficients defined by

$$\left.\begin{aligned}a_0&=C_{44}(C_{33}\epsilon_{33}+e_{33}^2),\\ b_0&=(e_{31}+e_{15})[2C_{13}e_{33}-C_{33}(e_{31}+e_{15})]+2C_{44}e_{33}e_{31}\\ &\quad -C_{11}e_{33}^2-\epsilon_{11}C_{33}C_{44}-\epsilon_{33}c^2,\\ c_0&=2e_{15}[C_{11}e_{33}-C_{13}(e_{31}+e_{15})]+C_{44}e_{31}^2+\\ &\quad \epsilon_{33}C_{11}C_{44}+\epsilon_{11}c^2,\\ d_0&=-C_{11}(C_{44}\epsilon_{11}+e_{15}^2),\\ c^2&=C_{11}C_{33}-C_{13}(C_{13}+2C_{44}).\end{aligned}\right\} \tag{17}$$

Using the operator theory, we obtain the general solution to the equations (1), as

$$\left.\begin{aligned}\widehat{u_r}(\xi,z)&=A_{i1}\hat{F}(\xi,z),\\ \widehat{u_z}(\xi,z)&=A_{i2}\hat{F}(\xi,z),\\ \hat{\Phi}(\xi,z)&=A_{i3}\hat{F}(\xi,z),\end{aligned}\right\} \tag{18}$$

Where A_{ij} are the algebraic cominors of the matrix operator and $\hat{F}(\xi,z)$ is the zero order Hankel transform of the general solution $F(r, z)$, satisfying the equations

$$\left.\begin{aligned}|\mathrm{A}|\hat{F}(\xi,z)&=0,\\ (D^2+\lambda_1^2\Delta)(D^2+\lambda_2^2\Delta)(D^2+\lambda_3^2\Delta)F(r,z)&=0.\end{aligned}\right\} \tag{19}$$

Here, $\Delta = \frac{\partial^2}{\partial r^2} + \frac{1}{r}\frac{\partial}{\partial r}$ and $D^2 = \frac{\partial^2}{\partial z^2}$.

Taking $i = 3$ and writing down the expression for A_{3i}, we obtain

$$\left.\begin{aligned} \widehat{u_r}(\xi, z) &= (a_1 D^2 + b_1\xi^2)\xi D\hat{F}(\xi, z), \\ \widehat{u_z}(\xi, z) &= -(a_2 D^4 + b_2\xi^2 D^2 + c_2\xi^4)\hat{F}(\xi, z), \\ \hat{\phi}(\xi, z) &= (a_3 D^4 + b_3\xi^2 D^2 + c_3\xi^4)\hat{F}(\xi, z), \end{aligned}\right\} \tag{20}$$

where

$$\left.\begin{aligned} a_1 &= C_{33}(e_{31} + e_{15}) - (C_{13} + C_{44})e_{33}, \quad b_1 = C_{13}e_{15} - C_{44}e_{31}, \\ a_2 &= C_{44}e_{33}, \qquad b_2 = (C_{13} + C_{44})e_{31} + C_{13}e_{15} - C_{11}e_{33}, \\ c_2 &= C_{11}e_{15}, \qquad a_3 = C_{44}C_{33}, \\ b_3 &= C_{13}^2 + 2C_{13}C_{44} - C_{11}C_{33}, \qquad c_3 = C_{11}C_{44}. \end{aligned}\right\} \tag{21}$$

The inverse Hankel transforms to equation (20) yield

$$\left.\begin{aligned} u_r(r, z) &= -(a_1 D^2 - b_1\Delta)\frac{\partial^2}{\partial r \partial z}F(r, z), \\ u_z(r, z) &= -(a_2 D^4 - b_2\Delta D^2 + c_2\Delta^2)F(r, z), \\ \Phi(r, z) &= (a_3 D^4 - b_3\Delta D^2 + c_3\Delta^2)F(r, z). \end{aligned}\right\} \tag{22}$$

Using the generalized Almansi's theorem [22], the function $F(r, z)$, which satisfies equation $(19)_2$, can be expressed in terms of three quasi-harmonic functions

$$F = \begin{cases} F_1 + F_2 + F_3 & \text{for distinct } \lambda_i, \\ F_1 + F_2 + zF_3 & \text{for } \lambda_1 \neq \lambda_2 = \lambda_3, \\ F_1 + zF_2 + z^2F_3 & \text{for } \lambda_1 = \lambda_2 = \lambda_3, \end{cases} \tag{23}$$

where $F_i(r, z)$ satisfies

$$\left(\Delta + \frac{1}{\lambda_i^2 D^2}\right)F_i(r, z) = 0, \; i = 1, 2, 3. \tag{24}$$

As we shall see later that the roots of equation (16) are all distinct in our considered problem, so we shall consider only first solution in equation (23). Using

$$\Delta F_i = -\frac{1}{\lambda_i^2}D^2 F_i,$$

and summing in equations (22), we obtain

$$\left.\begin{aligned} u_r(r, z) &= -\sum_{i=1}^{3}\alpha_{i1}\frac{\partial^4 F_i}{\partial r \partial z^3}, \\ u_z(r, z) &= -\sum_{i=1}^{3}\alpha_{i2}\frac{\partial^4 F_i}{\partial z^4}, \\ \phi(r, z) &= \sum_{i=1}^{3}\alpha_{i3}\frac{\partial^4 F_i}{\partial z^4}, \end{aligned}\right\} \tag{25}$$

The coefficients α_{ij} are

$$\alpha_{ij} = a_j + \frac{b_j}{\lambda_i^2} + \frac{c_j}{\lambda_i^4},$$

where a_j, b_j and c_j are defined by equations (21) and $c_1 = 0$. If we assumed that

$$\alpha_{i2}\frac{\partial^3}{\partial z^3}F_i(r,z) = -\frac{1}{\lambda_i}\varphi_i(r,z),$$

then equations (25) can be further simplified to

$$\left.\begin{aligned} u_r(r,z) &= \sum_{i=1}^{3} a_{i1}\lambda_i \frac{\partial \varphi_i}{\partial r}, \\ u_z(r,z) &= \sum_{i=1}^{3} \frac{1}{\lambda_i}\frac{\partial \varphi_i}{\partial z}, \\ \phi(r,z) &= -\sum_{i=1}^{3} \frac{a_{i3}}{\lambda_i}\frac{\partial \varphi_i}{\partial z}, \end{aligned}\right\} \tag{26}$$

where

$$\left.\begin{aligned} a_{i1} &= \frac{\alpha_{i1}}{\alpha_{i2}}\frac{1}{\lambda_i^2} = \frac{a_1\lambda_i^2 + b_1}{a_2\lambda_i^4 + b_2\lambda_i^2 + c_2^2}, \\ a_{i3} &= \frac{\alpha_{i3}}{\alpha_{i2}} = \frac{a_3\lambda_i^4 + b_3\lambda_i^2 + c_3}{a_2\lambda_i^4 + b_2\lambda_i^2 + c_2} = \frac{C_{13} + C_{44}}{e_{31} + e_{15}} - \frac{C_{11} - C_{44}\lambda_i^2}{e_{31} + e_{15}}a_{i1}, \end{aligned}\right\} \tag{27}$$

and for the quasi-harmonic function $\varphi_i(r,z)$

$$\left(\Delta + \frac{1}{\lambda_i^2}\frac{\partial^2}{\partial z^2}\right)\varphi_i(r,z) = 0. \tag{28}$$

The relationships between stress, displacement and electric potential for a transversely isotropic piezoelectric medium, in the case of axial symmetry, are

$$\begin{bmatrix}\sigma_{rr}\\ \sigma_{\theta\theta}\\ \sigma_{zz}\\ \sigma_{zr}\end{bmatrix} = \begin{bmatrix} C_{11} & C_{12} & 0 & 0 & C_{13} & 0 & e_{31} \\ C_{12} & C_{11} & 0 & 0 & C_{13} & 0 & e_{31} \\ C_{13} & C_{13} & 0 & 0 & C_{33} & 0 & e_{33} \\ 0 & 0 & C_{44} & C_{44} & 0 & e_{15} & 0 \end{bmatrix} \begin{bmatrix} u_{r,r} \\ \frac{u_r}{r} \\ u_{r,z} \\ u_{z,r} \\ u_{z,z} \\ \phi_r \\ \phi_z \end{bmatrix}. \tag{29}$$

Substituting equations (26) into equations (29), we obtain

$$\left.\begin{aligned} \sigma_{rr}(r,z) &= -\sum_{i=1}^{3}\frac{a_{i4}}{\lambda_i}\frac{\partial^2\varphi_i}{\partial z^2} - (C_{11} - C_{12})\frac{u_r}{r}, \quad \sigma_{zz}(r,z) = \sum_{i=1}^{3}\frac{a_{i4}}{\lambda_i^3}\frac{\partial^2\varphi_i}{\partial z^2}, \\ \sigma_{\theta\theta}(r,z) &= -\sum_{i=1}^{3}\frac{a_{i4}}{\lambda_i^2}\frac{\partial^2\varphi_i}{\partial z^2} - (C_{11} - C_{12})\frac{\partial u_r}{\partial r}, \quad \sigma_{zr}(r,z) = \sum_{i=1}^{3}\frac{a_{i4}}{\lambda_i}\frac{\partial^2\varphi_i}{\partial r\partial z}, \end{aligned}\right\} \tag{30}$$

where

$$a_{i4} = \frac{e_{31}C_{44}\lambda_i^2 + e_{15}C_{11}}{e_{31} + e_{15}}a_{i1} + \frac{C_{44}e_{31} - C_{13}e_{15}}{e_{31} + e_{15}}. \tag{31}$$

The components of the electric field vector E_r and E_z are obtained from relations

$$\left.\begin{aligned} E_r &= -\frac{\partial \phi}{\partial r} = \sum_{i=1}^{3} \frac{a_{i3}}{\lambda_i} \frac{\partial^2 \varphi_i}{\partial r \partial z}, \\ E_z &= -\frac{\partial \phi}{\partial z} = \sum_{i=1}^{3} \frac{a_{i3}}{\lambda_i} \frac{\partial^2 \varphi_i}{\partial z^2}. \end{aligned}\right\} \tag{32}$$

The electric displacements are defined by equations

$$\begin{bmatrix} D_r \\ D_z \end{bmatrix} = \begin{bmatrix} 0 & 0 & e_{15} & e_{15} & 0 & \epsilon_{11} & 0 \\ e_{31} & e_{31} & 0 & 0 & e_{33} & 0 & \epsilon_{33} \end{bmatrix} \begin{bmatrix} u_{r,r} \\ \frac{u_r}{r} \\ u_{r,z} \\ u_{z,r} \\ u_{z,z} \\ E_r \\ E_z \end{bmatrix}. \tag{33}$$

In terms of φ_i,

$$\left.\begin{aligned} D_r &= \sum_{i=1}^{3} a_{i5} \lambda_i \frac{\partial^2 \varphi_i}{\partial r \partial z}, \\ D_z &= \sum_{i=1}^{3} \frac{a_{i5}}{\lambda_i} \frac{\partial^2 \varphi_i}{\partial z^2}, \end{aligned}\right\} \tag{34}$$

where

$$a_{i5} = \frac{e_{33}\epsilon_{11} - e_{15}\epsilon_{33}}{\epsilon_{11} - \epsilon_{33}\lambda_i^2} - \frac{e_{31}\epsilon_{11} - e_{15}\epsilon_{33}\lambda_i^2}{\epsilon_{11} - \epsilon_{33}\lambda_i^2}\, a_{i1}\,. \tag{35}$$

It can be easily verified that:
Gauss' law [16]

$$\frac{\partial D_r}{\partial r} + \frac{D_r}{r} + \frac{\partial D_z}{\partial z} = 0, \tag{36}$$

and equilibrium equations for stresses [14]

$$\left.\begin{aligned} \frac{\partial \sigma_{rr}}{\partial r} + \frac{\partial \sigma_{rz}}{\partial z} + \frac{\sigma_{rr} - \sigma_{\theta\theta}}{r} &= 0, \\ \frac{\partial \sigma_{zr}}{\partial r} + \frac{\partial \sigma_{zz}}{\partial z} + \frac{\sigma_{zr}}{r} &= 0. \end{aligned}\right\} \tag{37}$$

are satisfied.

In the vacuum, constitutive equations (33) and governing equations (36) become

$$\left.\begin{aligned} D_r = \epsilon_0 E_r, \qquad D_z = \epsilon_0 E_z, \\ \frac{\partial^2 \phi}{\partial r^2} + \frac{1}{r}\frac{\partial \phi}{\partial r} + \frac{\partial^2 \phi}{\partial z^2} = 0, \end{aligned}\right\} \tag{38}$$

where ϵ_0 is the electric permittivity of the vacuum.
For axially symmetric problems, the general solution of the differential equation (28) may be written as

$$\varphi_i(r,z) = \int_0^\infty \left[A_i(\xi)e^{-\lambda_i \xi z} + B_i(\xi)e^{\lambda_i \xi z}\right] J_0(r\xi)d\xi, \tag{39}$$

where $A_i(\xi), B_i(\xi), (i = 1,2,3)$ are arbitrary functions of the transform parameter ξ, which are to be determined from the boundary conditions (2)-(10) and λ_i are the roots of equation (16).

Using equations (39), (26) and (30) into the boundary conditions (2) − (10) we obtain

$$\sum_{i=1}^{3} \int_0^\infty [A_i(\xi) - B_i(\xi)]\xi^2 J_1(r\xi)d\xi = f(r), \quad 0 \le r < \infty, \tag{40}$$

$$\sum_{i=1}^{3} a_{i4}[A_i(\xi) - B_i(\xi)] = 0, \quad 0 \le r < \infty, \tag{41}$$

$$\sum_{i=1}^{3} \frac{a_{i4}}{\lambda_i} \int_0^\infty \left[A_i(\xi)e^{-\lambda_i \xi h} + B_i(\xi)e^{\lambda_i \xi h}\right]\xi^2 J_0(r\xi)d\xi = \mp \frac{P}{2\pi a}\delta(r-a), \quad 0 \le r < \infty, \tag{42}$$

$$\sum_{i=1}^{3} \frac{a_{i4}}{\lambda_i} \int_0^\infty [A_i(\xi) + B_i(\xi)]\xi^2 J_0(r\xi)d\xi = -p_0, \quad 0 \le r \le b, \tag{43}$$

$$\sum_{i=1}^{3} a_{i4}\left[A_i(\xi)e^{-\lambda_i \xi h} - B_i(\xi)e^{\lambda_i \xi h}\right] = 0, \quad 0 \le r < \infty, \tag{44}$$

$$\sum_{i=1}^{3} \int_0^\infty a_{i5}\lambda_i [A_i(\xi) + B_i(\xi)]\xi^2 J_0(r\xi)d\xi = 0, \quad |r| > b, \tag{45}$$

$$\sum_{i=1}^{3} \int_0^\infty a_{i3}[A_i(\xi) - B_i(\xi)]\xi J_0(r\xi)d\xi = 0, \quad 0 \le r \le b, \tag{46}$$

$$\sum_{i=1}^{3} \int_0^\infty a_{i3}\left[A_i(\xi)e^{-\lambda_i \xi h} - B_i(\xi)e^{\lambda_i \xi h}\right]\xi J_0(r\xi)d\xi = \phi_0, \quad r \ge 0, \tag{47}$$

$$\sum_{i=1}^{3} \int_0^\infty a_{i3}[-A_i(\xi) + B_i(\xi)]\xi^2 J_1(r\xi)d\xi = 0, \quad |r| > b. \tag{48}$$

On inverse Hankel transform, equations (40) and (42) become

$$\sum_{i=1}^{3}[A_i(\xi) - B_i(\xi)] = F_1(\xi), \quad 0 \le r < \infty, \tag{49}$$

and

$$\sum_{i=1}^{3}\frac{a_{i4}}{\lambda_i}\left[A_i(\xi)e^{-\lambda_i\xi h} + B_i(\xi)e^{\lambda_i\xi h}\right] = R, \qquad 0 \le r < \infty, \tag{50}$$

respectively, where

$$F_1(\xi) = \frac{1}{\xi}\int_0^{\infty} rf(r)J_1(r\xi)dr, \tag{51}$$

and

$$R = \mp\frac{P}{2\pi\xi}J_0(a\xi), \tag{52}$$

Taking derivative with respect to r, the equation (47) becomes

$$\sum_{i=1}^{3}a_{i3}\left[A_i(\xi)e^{-\lambda_i\xi h} - B_i(\xi)e^{\lambda_i\xi h}\right] = 0, \quad |r| \ge 0. \tag{53}$$

Equations (49), (41) and (44), (53) yield

$$A_1(\xi) = \chi_7(\xi)F_1(\xi) + \chi_8(\xi)A_3(\xi) + \chi_9(\xi)B_3(\xi), \tag{54}$$
$$B_1(\xi) = \chi_{10}(\xi)F_1(\xi) + \chi_{11}(\xi)A_3(\xi) + \chi_{12}(\xi)B_3(\xi), \tag{55}$$
$$A_2(\xi) = \chi_{13}(\xi)F_1(\xi) + \chi_{14}(\xi)A_3(\xi) + \chi_{15}(\xi)B_3(\xi), \tag{56}$$
$$B_2(\xi) = \chi_{16}(\xi)F_1(\xi) + \chi_{17}(\xi)A_3(\xi) + \chi_{18}(\xi)B_3(\xi), \tag{57}$$

where

$$\chi_1 = \frac{a_{24}}{a_{24} - a_{14}}, \quad \chi_2 = \frac{a_{34} - a_{24}}{a_{24} - a_{14}}, \quad \chi_3 = -\frac{a_{14}}{a_{24} - a_{14}}, \quad \chi_4 = \frac{a_{14} - a_{34}}{a_{24} - a_{14}},$$

$$\chi_5 = \frac{-a_{34}a_{23} + a_{33}a_{24}}{a_{14}a_{23} - a_{13}a_{24}}, \chi_6 = \frac{-a_{14}a_{33} + a_{13}a_{34}}{a_{14}a_{23} - a_{13}a_{24}}, \chi_7(\xi) = \frac{\chi_1}{1 - e^{-2\lambda_1\xi h}},$$

$$\chi_8(\xi) = \frac{\chi_2 - \chi_5 e^{-(\lambda_1+\lambda_3)\xi h}}{1 - e^{-2\lambda_1\xi h}}, \quad \chi_9(\xi) = \frac{-\chi_2 + \chi_5 e^{(\lambda_3-\lambda_1)\xi h}}{1 - e^{-2\lambda_1\xi h}},$$

$$\chi_{10}(\xi) = \frac{\chi_1}{-1 + e^{2\lambda_1\xi h}}, \quad \chi_{11}(\xi) = \frac{\chi_2 - \chi_5 e^{(\lambda_1-\lambda_3)\xi h}}{-1 + e^{2\lambda_1\xi h}},$$

$$\chi_{12}(\xi) = \frac{-\chi_2 + \chi_5 e^{(\lambda_1+\lambda_3)\xi h}}{-1 + e^{2\lambda_1\xi h}}, \quad \chi_{13}(\xi) = \frac{\chi_3}{1 - e^{-2\lambda_2\xi h}},$$
$$\chi_{14}(\xi) = \frac{\chi_4 - \chi_6 e^{-(\lambda_2+\lambda_3)\xi h}}{1 - e^{-2\lambda_2\xi h}}, \quad \chi_{15}(\xi) = \frac{-\chi_4 + \chi_6 e^{(\lambda_3-\lambda_2)\xi h}}{1 - e^{-2\lambda_2\xi h}},$$
$$\chi_{16}(\xi) = \frac{\chi_3}{-1 + e^{2\lambda_2\xi h}}, \quad \chi_{17}(\xi) = \frac{\chi_4 - \chi_6 e^{(\lambda_2-\lambda_3)\xi h}}{-1 + e^{2\lambda_2\xi h}},$$

$$\chi_{18}(\xi) = \frac{-\chi_4 + \chi_6 e^{(\lambda_2+\lambda_3)\xi h}}{-1 + e^{2\lambda_2 \xi h}}.$$

Equation (50) yields

$$B_3(\xi) = \chi_{22}(\xi)A_3(\xi) + \chi_{23}(\xi)F_1(\xi) + \chi_{24}(\xi)R, \tag{58}$$

where

$$\chi_{19}(\xi) = \frac{a_{14}}{\lambda_1}\chi_8(\xi)e^{-\lambda_1\xi h} + \frac{a_{14}}{\lambda_1}\chi_{11}(\xi)e^{\lambda_1\xi h} + \frac{a_{24}}{\lambda_2}\chi_{14}(\xi)e^{-\lambda_2\xi h} + \frac{a_{24}}{\lambda_2}\chi_{17}(\xi)e^{\lambda_2\xi h} + \frac{a_{34}}{\lambda_3}e^{-\lambda_3\xi h},$$

$$\chi_{20}(\xi) = \frac{a_{14}}{\lambda_1}\chi_9(\xi)e^{-\lambda_1\xi h} + \frac{a_{14}}{\lambda_1}\chi_{12}(\xi)e^{\lambda_1\xi h} + \frac{a_{24}}{\lambda_2}\chi_{15}(\xi)e^{-\lambda_2\xi h} + \frac{a_{24}}{\lambda_2}\chi_{18}(\xi)e^{\lambda_2\xi h} + \frac{a_{34}}{\lambda_3}e^{\lambda_3\xi h},$$

$$\chi_{21}(\xi) = \frac{a_{14}}{\lambda_1}\chi_7(\xi)e^{-\lambda_1\xi h} + \frac{a_{14}}{\lambda_1}\chi_{10}(\xi)e^{\lambda_1\xi h} + \frac{a_{24}}{\lambda_2}\chi_{13}(\xi)e^{-\lambda_2\xi h} + \frac{a_{24}}{\lambda_2}\chi_{16}(\xi)e^{\lambda_2\xi h},$$

$$\chi_{22}(\xi) = -\frac{\chi_{19}(\xi)}{\chi_{20}(\xi)}, \quad \chi_{23}(\xi) = -\frac{\chi_{21}(\xi)}{\chi_{20}(\xi)}, \quad \chi_{24}(\xi) = -\frac{1}{\chi_{20}(\xi)}.$$

Using equations (54) − (57) in equation (45) we get,

$$\int_0^\infty [\chi_{25}(\xi)A_3(\xi) + \chi_{26}(\xi)F_1(\xi) + \chi_{27}(\xi)R]\xi^2 J_0(r\xi)d\xi = 0, \qquad |r| > b, \tag{59}$$

where

$$\begin{aligned}\chi_{25}(\xi) = {} & \lambda_1 a_{15}[\chi_8(\xi) + \chi_9(\xi)\chi_{22}(\xi) + \chi_{11}(\xi) + \chi_{12}(\xi)\chi_{22}(\xi)] \\ & + \lambda_2 a_{25}[\chi_{14}(\xi) + \chi_{15}(\xi)\chi_{22}(\xi) + \chi_{17}(\xi) + \chi_{18}(\xi)\chi_{22}(\xi)] \\ & + \lambda_3 a_{35}[1 + \chi_{22}(\xi)],\end{aligned}$$

$$\begin{aligned}\chi_{26}(\xi) = {} & \lambda_1 a_{15}[\chi_7(\xi) + \chi_9(\xi)\chi_{23}(\xi) + \chi_{10}(\xi) + \chi_{12}(\xi)\chi_{23}(\xi)] \\ & + \lambda_2 a_{25}[\chi_{13}(\xi) + \chi_{15}(\xi)\chi_{23}(\xi) + \chi_{16}(\xi) + \chi_{18}(\xi)\chi_{23}(\xi)] \\ & + \lambda_3 a_{35}\chi_{23}(\xi),\end{aligned}$$

$$\begin{aligned}\chi_{27}(\xi) = {} & \lambda_1 a_{15}[\chi_9(\xi)\chi_{24}(\xi) + \chi_{12}(\xi)\chi_{24}(\xi)] + \lambda_2 a_{25}[\chi_{15}(\xi)\chi_{24}(\xi) \\ & + \chi_{18}(\xi)\chi_{24}(\xi)] + \lambda_3 a_{35}\chi_{24}(\xi).\end{aligned}$$

Now we assume that

$$\{\chi_{25}(\xi)A_3(\xi) + \chi_{26}(\xi)F_1(\xi) + \chi_{27}(\xi)R\}\xi = \sqrt{\frac{2}{\pi}}\int_0^b \phi_1(x)\cos(\xi x)\,dx. \tag{60}$$

Then equation (59) is automatically satisfied. Use of equations (54) − (57) into (48) leads

$$\int_0^\infty [\chi_{28}(\xi)A_3(\xi) + \chi_{29}(\xi)F_1(\xi) + \chi_{30}(\xi)R]\xi^2 J_1(r\xi)d\xi = 0, \qquad |r| > b, \quad (61)$$

where

$$\begin{aligned}
\chi_{28}(\xi) &= a_{13}[-\chi_8(\xi) - \chi_9(\xi)\chi_{22}(\xi) + \chi_{11}(\xi) + \chi_{12}(\xi)\chi_{22}(\xi)] \\
&\quad + a_{23}[-\chi_{14}(\xi) - \chi_{15}(\xi)\chi_{22}(\xi) + \chi_{17}(\xi) + \chi_{18}(\xi)\chi_{22}(\xi)] \\
&\quad + a_{33}[-1 + \chi_{22}(\xi)], \\
\chi_{29}(\xi) &= a_{13}[-\chi_7(\xi) - \chi_9(\xi)\chi_{23}(\xi) + \chi_{10}(\xi) + \chi_{12}(\xi)\chi_{23}(\xi)] \\
&\quad + a_{23}[-\chi_{13}(\xi) - \chi_{15}(\xi)\chi_{23}(\xi) + \chi_{16}(\xi) + \chi_{18}(\xi)\chi_{23}(\xi)] \\
&\quad + a_{33}\chi_{23}(\xi), \\
\chi_{30}(\xi) &= a_{13}[-\chi_9(\xi)\chi_{24}(\xi) + \chi_{12}(\xi)\chi_{24}(\xi)] + a_{23}[-\chi_{15}(\xi)\chi_{24}(\xi) \\
&\quad + \chi_{18}(\xi)\chi_{24}(\xi)] + a_{33}\chi_{24}(\xi).
\end{aligned}$$

Now we assume that

$$\{\chi_{28}(\xi)A_3(\xi) + \chi_{29}(\xi)F_1(\xi) + \chi_{30}(\xi)R\}\xi = \sqrt{\frac{2}{\pi}}\int_0^b \frac{1}{x}\phi_2(x)\sin(\xi x)\,dx. \quad (62)$$

Then equation (61) is automatically satisfied. Solving equations (60) and (62) we get

$$\begin{aligned}
A_3(\xi) &= \beta_1(\xi)\sqrt{\frac{2}{\pi}}\int_0^b \phi_1(x)\cos(\xi x)\,dx \\
&\quad + \beta_2(\xi)\sqrt{\frac{2}{\pi}}\int_0^b \frac{1}{x}\phi_2(x)\sin(\xi x)\,dx + \beta_3(\xi)R, \quad (63)
\end{aligned}$$

and

$$\begin{aligned}
F_1(\xi) &= \beta_4(\xi)\sqrt{\frac{2}{\pi}}\int_0^b \phi_1(x)\cos(\xi x)\,dx \\
&\quad + \beta_5(\xi)\sqrt{\frac{2}{\pi}}\int_0^b \frac{1}{x}\phi_2(x)\sin(\xi x)\,dx + \beta_6(\xi)R, \quad (64)
\end{aligned}$$

where

$$\beta_1(\xi) = \frac{\chi_{29}(\xi)}{\{\chi_{25}(\xi)\chi_{29}(\xi) - \chi_{26}(\xi)\chi_{28}(\xi)\}\xi},$$

$$\beta_2(\xi) = -\frac{\chi_{26}(\xi)}{\{\chi_{25}(\xi)\chi_{29}(\xi) - \chi_{26}(\xi)\chi_{28}(\xi)\}\xi},$$

$$\beta_3(\xi) = \frac{\chi_{26}(\xi)\chi_{30}(\xi) - \chi_{27}(\xi)\chi_{29}(\xi)}{\{\chi_{25}(\xi)\chi_{29}(\xi) - \chi_{26}(\xi)\chi_{28}(\xi)\}},$$

$$\beta_4(\xi) = -\frac{\chi_{28}(\xi)}{\{\chi_{25}(\xi)\chi_{29}(\xi) - \chi_{26}(\xi)\chi_{28}(\xi)\}\xi},$$

$$\beta_5(\xi) = \frac{\chi_{25}(\xi)}{\{\chi_{25}(\xi)\chi_{29}(\xi) - \chi_{26}(\xi)\chi_{28}(\xi)\}\xi},$$

$$\beta_6(\xi) = \frac{\chi_{27}(\xi)\chi_{28}(\xi) - \chi_{25}(\xi)\chi_{30}(\xi)}{\{\chi_{25}(\xi)\chi_{29}(\xi) - \chi_{26}(\xi)\chi_{28}(\xi)\}},$$

From equations (43), (54) − (57) we get

$$\int_0^\infty [\chi_{31}(\xi)A_3(\xi) + \chi_{32}(\xi)F_1(\xi) + \chi_{33}(\xi)R]\xi^2 J_0(r\xi)d\xi = -p_0, \quad 0 \le r \le b, \qquad (65)$$

where

$$\chi_{31}(\xi) = \frac{a_{14}}{\lambda_1}[\chi_8(\xi) + \chi_9(\xi)\chi_{22}(\xi) + \chi_{11}(\xi) + \chi_{12}(\xi)\chi_{22}(\xi)] + \frac{a_{24}}{\lambda_2}[\chi_{14}(\xi) + \chi_{15}(\xi)\chi_{22}(\xi) + \chi_{17}(\xi) + \chi_{18}(\xi)\chi_{22}(\xi)] + \frac{a_{34}}{\lambda_3}[1 + \chi_{22}(\xi)],$$

$$\chi_{32}(\xi) = \frac{a_{14}}{\lambda_1}[\chi_7(\xi) + \chi_9(\xi)\chi_{23}(\xi) + \chi_{10}(\xi) + \chi_{12}(\xi)\chi_{23}(\xi)] + \frac{a_{24}}{\lambda_2}[\chi_{13}(\xi) + \chi_{15}(\xi)\chi_{23}(\xi) + \chi_{16}(\xi) + \chi_{18}(\xi)\chi_{23}(\xi)] + \frac{a_{34}}{\lambda_3}\chi_{23}(\xi),$$

$$\chi_{33}(\xi) = \frac{a_{14}}{\lambda_1}[\chi_9(\xi)\chi_{24}(\xi) + \chi_{12}(\xi)\chi_{24}(\xi)] + \frac{a_{24}}{\lambda_2}[\chi_{15}(\xi)\chi_{24}(\xi) + \chi_{18}(\xi)\chi_{24}(\xi)] + \frac{a_{34}}{\lambda_3}\chi_{24}(\xi).$$

Again equation (65) with the help of equations (63),(64) yields

$$\int_0^b \Phi_1(x)k_{11}(r,x)dx + \int_0^b \Phi_2(x)k_{12}(r,x)dx = -p_0 - \int_0^\infty \chi_{34}(\xi)R\xi^2 J_0(r\xi)d\xi, \quad 0 \le r \le b, \qquad (66)$$

where

$$k_{11}(r,x) = \int_0^\infty G_1(\xi)\xi^2 J_0(r\xi)cos(\xi x)d\xi,$$

$$k_{12}(r,x) = \int_0^\infty \frac{1}{x}G_2(\xi)\xi^2 J_0(r\xi)sin(\xi x)d\xi,$$

$$G_1(\xi) = \sqrt{\frac{2}{\pi}}[\beta_1(\xi)\chi_{31}(\xi) + \beta_4(\xi)\chi_{32}(\xi)],$$

$$G_2(\xi) = \sqrt{\frac{2}{\pi}}[\beta_2(\xi)\chi_{31}(\xi) + \beta_5(\xi)\chi_{32}(\xi)],$$

$$\chi_{34}(\xi) = \beta_3(\xi)\chi_{31}(\xi) + \beta_6(\xi)\chi_{32}(\xi) + \chi_{33}(\xi).$$

Now equation (66) can be written as

$$\int_0^r \frac{dx}{\sqrt{r^2 - x^2}}[\Phi_1(x) + \int_0^b \Phi_1(u)L_1(u,x)du] = f_1(r), \quad (67)$$

which is an Abel type integral equation, where

$$f_1(r) = p_0 - \int_0^\infty \chi_{34}(\xi)R\xi^2 J_0(r\xi)d\xi - \int_0^b \Phi_2(u)k_{12}(r,u)du,$$

$$L_1(u,x) = \frac{2}{\pi}\int_0^\infty H_1(\xi)cos(\xi u)cos(\xi x)d\xi, \; H_1(\xi) = \xi^2 G_1(\xi) - 1.$$

After some work we get the integral equation in Φ_1 as

$$\Phi_1(x) + \int_0^b \Phi_1(u)L_1(u,x)du + \int_0^b \Phi_2(u)L_2(u,x)du = -\frac{2p_0}{\pi} - L_3(u,x),$$

$$0 \le x \le b, \quad (68)$$

where

$$L_2(u,x) = -\frac{2}{\pi}\int_0^\infty G_2(\xi)\xi^2 \frac{\cos(\xi x)}{u}\sin(\xi u)d\xi,$$

$$L_3(u,x) = \frac{2}{\pi}\int_0^\infty \chi_{34}(\xi)R\xi^2 cos(\xi x)\, sin(\xi u)d\xi.$$

Taking derivative of equation (46) with respect to r and using equations (63), (64) we get

$$\int_0^b \Phi_1(x)k_{21}(r,x)dx + \int_0^b \Phi_2(x)k_{22}(r,x)dx = -\int_0^\infty \chi_{38}(\xi)R\xi^2 J_1(r\xi)d\xi,$$

$$0 \le r \le b, \quad (69)$$

where

$$k_{21}(r,x) = \int_0^\infty G_3(\xi)\xi^2 J_1(r\xi)cos(\xi x)d\xi, \; k_{22}(r,x) = \int_0^\infty \frac{1}{x}G_4(\xi)\xi^2 J_1(r\xi)sin(\xi x)d\xi,$$

$$G_3(\xi) = \sqrt{\frac{2}{\pi}}[\beta_1(\xi)\chi_{35}(\xi) + \beta_4(\xi)\chi_{36}(\xi)],$$

$$G_4(\xi) = \sqrt{\frac{2}{\pi}}[\beta_2(\xi)\chi_{35}(\xi) + \beta_5(\xi)\chi_{36}(\xi)],$$

$$\chi_{35}(\xi) = a_{13}[\chi_8(\xi) + \chi_9(\xi)\chi_{22}(\xi) - \chi_{11}(\xi) - \chi_{12}(\xi)\chi_{22}(\xi)] + a_{23}[\chi_{14}(\xi) + \chi_{15}(\xi)\chi_{22}(\xi) - \chi_{17}(\xi) - \chi_{18}(\xi)\chi_{22}(\xi)] + a_{33}[1 - \chi_{22}(\xi)],$$

$$\chi_{36}(\xi) = a_{13}[\chi_7(\xi) + \chi_9(\xi)\chi_{23}(\xi) - \chi_{10}(\xi) - \chi_{12}(\xi)\chi_{23}(\xi)] + a_{23}[\chi_{13}(\xi) + \chi_{15}(\xi)\chi_{23}(\xi) - \chi_{16}(\xi) - \chi_{18}(\xi)\chi_{23}(\xi)] - a_{33}\chi_{23}(\xi),$$

$$\chi_{37}(\xi) = a_{13}[\chi_9(\xi)\chi_{24}(\xi) - \chi_{12}(\xi)\chi_{24}(\xi)] + a_{23}[\chi_{15}(\xi)\chi_{24}(\xi) - \chi_{18}(\xi)\chi_{24}(\xi)] - a_{33}\chi_{24}(\xi),$$

$$\chi_{38}(\xi) = \beta_3(\xi)\chi_{35}(\xi) + \beta_6(\xi)\chi_{36}(\xi) + \chi_{37}(\xi).$$

Now equation (69) can be written as

$$\int_0^r \frac{dx}{\sqrt{r^2 - x^2}}[\Phi_2(x) + \int_0^b \Phi_2(u)L_4(u,x)du] = f_2(r), \quad 0 \le r \le b, \qquad (70)$$

which is an Abel type integral equation, where

$$f_2(r) = -r\int_0^b \phi_1(x)k_{12}(r,x)dx - r\int_0^\infty \chi_{38}(\xi)R\xi^2 J_1(r\xi)d\xi,$$

$$L_4(u,x) = \frac{2}{\pi}\int_0^\infty \frac{x}{u}H_2(\xi)sin(\xi u)sin(\xi x)d\xi, \quad H_2(\xi) = G_4(\xi)\xi^2 - 1.$$

After some work we get the integral equation in Φ_2 as

$$\Phi_2(x) + \int_0^b \Phi_1(u)L_5(u,x)du + \int_0^b \Phi_2(u)L_4(u,x)du = -L_6(u,x), \quad 0 \le x \le b, \quad (71)$$

where

$$L_5(u,x) = \int_0^\infty \sqrt{\frac{8x\xi^3}{\pi}}G_3(\xi)cos(\xi x)cos(\xi u)J_{\frac{3}{2}}(d\xi)d\xi,$$

$$L_6(u,x) = \int_0^\infty \sqrt{\frac{8x\xi^3}{\pi}}\chi_{38}(\xi)RJ_{\frac{3}{2}}(\xi x)d\xi.$$

Before further proceeding it will be convenient to introduce non-dimensional variables u', x', and r' by rescaling by length scale b:

$$u' = \frac{u}{b}, \quad x' = \frac{x}{b}, \quad r' = \frac{r}{b}. \qquad (72)$$

For notational convenience, we shall use only dimensionless variables and shall ignore the dashes on the transformed non-dimensional variables and the integral equations (68) and (71) become

$$\Phi_1(x) + \int_0^1 \Phi_1(u)L_1(u,x)du + \int_0^1 \Phi_2(u)L_2(u,x)du = -1 \pm QL_3(u,x), \quad 0 \le x \le 1, \quad (73)$$

$$\Phi_2(x) + \int_0^1 \Phi_1(u)L_5(u,x)du + \int_0^1 \Phi_2(u)L_4(u,x)du = -L_6(u,x), \quad 0 \le x \le 1, \quad (74)$$

where Q is the load ratio defined as:

$$Q = \frac{P}{2\pi p_0 b^2}.$$

These equations determine functions Φ_1 and Φ_2.

3. Determination of stress intensity factor

Presence of a crack in a solid significantly affects the stress distribution compared to that when there is no crack. While the stress distribution in a solid with a crack in the region far away from the crack is not much disturbed, the stresses in the neighborhood of the crack tip assumes a very high magnitude. In order to predict whether the crack has a tendency to expand further, the stress intensity factor (SIF), a quantity of physical interest, has been defined in fracture mechanics. The load at which failure occurs is referred to as the fracture strength. The stress intensity factor is defined as

$$k(b) = \lim_{s\to 1} \sqrt{b(s-1)}\, \sigma_{zz}^*(\mathrm{s}, 0),$$

where

$$r = \frac{b}{2}(1 + \mathrm{s}).$$

Use of the equations (66) and (5) and after some manipulation, the expression for $k(b)$ is obtained as

$$\frac{k(b)}{\pi}\sqrt{\frac{2}{b}} = -\phi_1(1). \quad (75)$$

where $\Phi_1(1)$ can be found out from the numerical solutions of the equations (73) and (74). Following the method as in [9] we obtain the crack surface displacement in the form

$$v(r,0) = \int_{-b}^{r} f(r)dr, \quad (-b < r < b), \quad (76)$$

Taking the inversion of Hankel transform of equation (49) and using the equation (64) into the equation (76), we can express the dimensionless normal displacement as

$$v'(r',0) = \int_{-1}^{r'} \left[\int_0^\infty F_1(\xi)\xi^2 J_1(r'\xi)d\xi\right] dr', \quad (-1 < r' < 1). \quad (77)$$

which can be obtained numerically, using Simpson's $\frac{1}{3}$ integration formula

and the appropriate interpolation formula.

5. Numerical results and discussions

The present study shows how the presence of a crack in an anisotropic piezoelectric layer under applied line load affects stress distribution and crack surface displacement values and how the SIF is influenced by the anisotropic and piezoelectric character of the medium and also by the position of the applied load. Since these effects are not easily visible from our complex theoretical expressions, we have numerically solved the relevant equations based on the elastic and piezoelectric material parameter values for some specific materials. In our numerical computation we have considered the piezoelectric materials PZT-4 and PZT-5. The parameter values for PZT-4 [15] are

$$\left.\begin{array}{l} C_{11} = 13.90,\quad C_{33} = 11.30,\quad C_{44} = 2.56 \\ C_{12} = 7.78,\quad\quad C_{13} = 7.43, \end{array}\right\} (\times 10^{10}, in \quad N/m^2)$$

$$\begin{array}{l} e_{15} = 13.44,\quad e_{31} = -6.98,\quad e_{33} = 13.84,\quad (in \quad C/m^2) \\ \epsilon_{11} = 60.00,\quad \epsilon_{33} = 54.70,\qquad (\times 10^{10}, in \quad C/Vm). \end{array}$$

and those of PZT-5 [7] are

$$\left.\begin{array}{l} C_{11} = 12.60,\quad C_{33} = 11.70,\qquad C_{44} = 3.53 \\ C_{12} = 5.50,\quad\quad C_{13} = 5.30, \end{array}\right\} (\times 10^{10}, in \quad N/m^2)$$

$$\begin{array}{l} e_{15} = 17.00,\quad e_{31} = -6.50,\quad e_{33} = 23.30,\quad (in \quad C/m^2) \\ \epsilon_{11} = 151.00,\quad \epsilon_{33} = 130.00,\qquad (\times 10^{10}, in \quad C/Vm). \end{array}$$

Considering the piezoelectric material of the layer as PZT-4, the variation of normalized stress intensity factor with b/h are shown in Figs. 2(a, b) for both the cases of applied compressive and tensile line loadings.

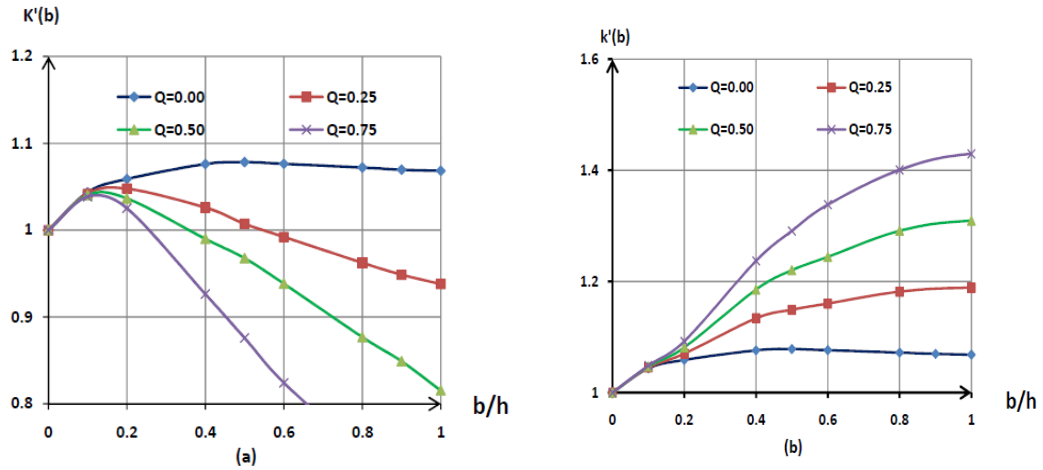

Fig.2 (a) Variation of normalized stress-intensity factor $k'(b)$ with b/h for various values of Q in the case of compressive line load $(a/b = 0.75)$. (b)Variation of normalized stress-intensity factor $k'(b)$ with b/h for various values of Q in the case of tensile line load $(a/b = 0.75)$.

It is observed from Fig.2(a) that for compressive line loading the normalized stress-intensity factor $k'(b)$ decreases with the increase of the load ratio Q and the increase of $k'_b(b)$ is quite significant for smaller values of Q. It is also observed from Fig.2(a) that the load ratio Q does not have much effect on the stress intensity factor $k'(b)$ for sufficiently small values of crack radius. Fig 2(b) represents the variations of $k'(b)$ with crack length under tensile nature of line loading. Contrary to the previous case it is observed that $k'(b)$ increases with Q.For small crack radius, the behavior of $k'(b)$ is similar to the case of compressive line loading.

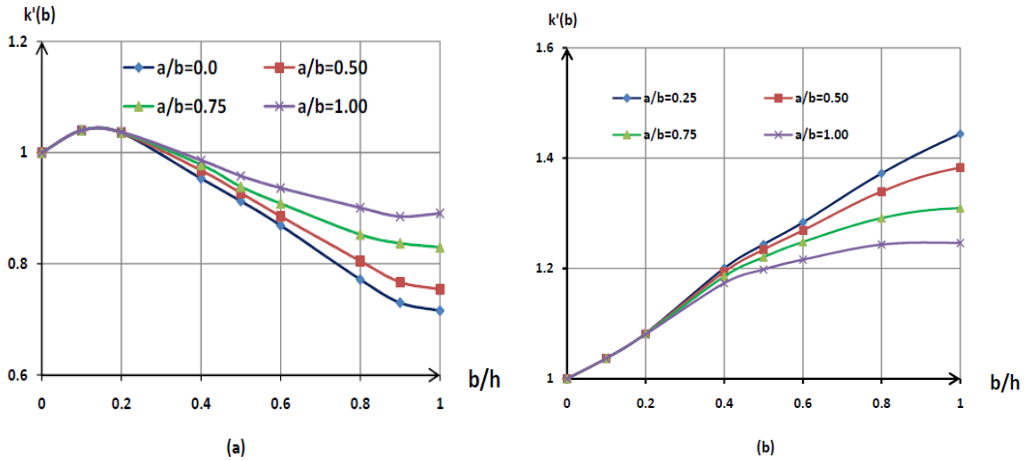

Fig.3 (a) Variation of normalized stress-intensity factor $k'(b)$for different values a/b in the case of compressive line load($Q = 0.5$). **(b)** Variation of normalized stress-intensity factor $k'(b)$ for different values of a/b in the case of tensile line load ($Q = 0.5$).

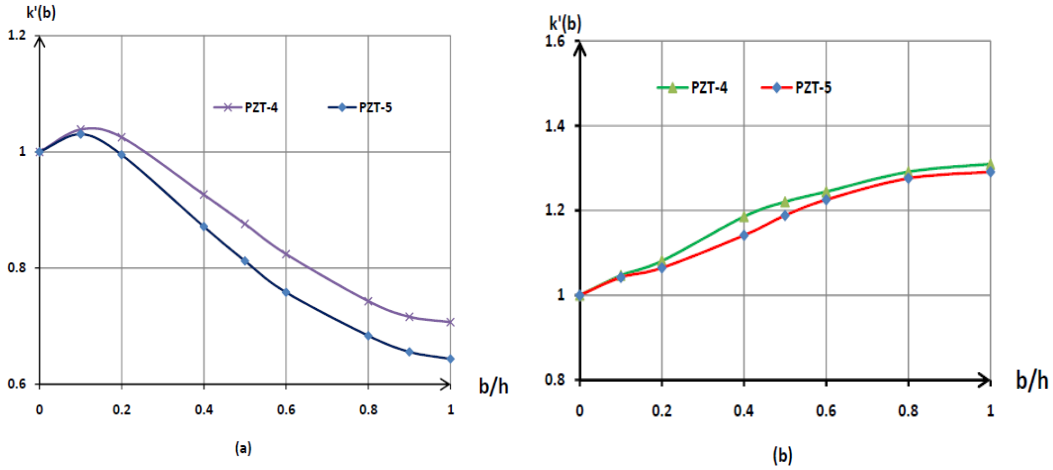

Fig.4 (a) Variation of normalized stress-intensity factor $k'(b)$ with b/h for various ceramics in the case of compressive line load ($a/b = 0.75, Q = 0.75$). **(b)** Variation of normalized stress-intensity factor $k'(b)$ with b/h for various ceramics in the case of tensile line load ($a/b = 0.75, Q = 0.50$).

Figs. 3(a, b) display the variations of normalized stress-intensity factor

$k'(b)$ for different line loading radius. It is noted that in the case of compressive line loading, $k'(b)$ increases with increasing $\frac{a}{b}$, but it decreases in the case of tensile line loading. In Figs. 4(a, b) normalized stress intensity factor experiences the effect of piezoelectric behavior under applied compressive and tensile line loadings corresponding to load ratio values $Q = 0.75$ and $Q = 0.50$ respectively. The normalized SIF are similar in behavior in respect of variation of crack radius but PZT-5 showing relatively smaller values.

Variations of normalized crack surface displacement $v'(r,0)$ with $\frac{r}{b}$ for different values of load ratio Q are displayed in Figs 5(a, b). It is clear from Fig. 5(a) that crack surface displacement $v'(r,0)$ decreases as load ratio Q increases for compressive loading, while for tensile loading the result is just the opposite. As expected, symmetry in elastic and piezoelectric behavior together with symmetry in applied loading yield crack surface displacement symmetrical with respect to the center of the crack.

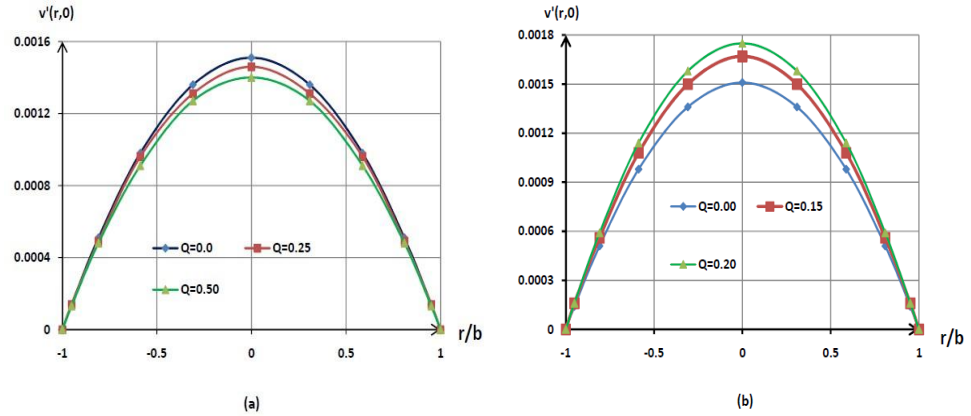

Fig.5 (a) Variation of normalized crack surface displacement $v'(r,0)$ for various values of Q in the case of compressive line load $(a/b = 0.25, b/h = 0.75)$. **(b)** Variation of normalized crack surface displacement $v'(r,0)$ for various values of Q in the case of tensile line load $(a/b = 0.25, b/h = 0.75)$.

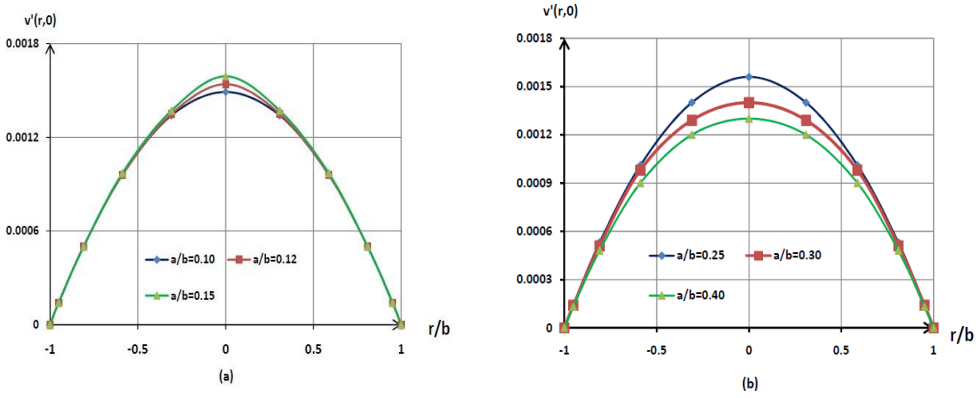

Fig.6 (a) Variation of normalized crack surface displacement $v'(r,0)$ for various values of Q in the case of compressive line load $(Q = 0.5, b/h = 0.75)$.**(b)** Variation of normalized crack surface displacement $v'(r,0)$ for various values of Q in the case of tensile line load $(Q = 0.20, b/h = 0.75)$.

Figs.6(a, b) illustrate the role of the radius of the applied loading circle on the normalized crack surface displacement for particular values of $\frac{b}{h} = 0.75$ and load ratio $Q = 0.50$ for compressive loading and $Q = 0.20$ for tensile loading.

It is observed in Fig 6(a) that for compressive loading the normalized crack surface displacement increases with the increased values of $\frac{a}{b}$ but behavior is just the opposite (Fig. 6(b)) for tensile loading. The effects of piezoelectric behavior on normalized crack surface displacement $v'(r,0)$ are shown in Figs. 7(a, b) taking $\frac{a}{b} = 0.25$, $\frac{b}{h} = 0.75$ and load ratio $Q = 0.50$ and $Q = 0.20$ for compressive and tensile loadings respectively. As expected it is observed from Figs. 5-7, that the normalized crack surface displacement $v'(r,0)$ assumes its maximum magnitude near the center of the crack.

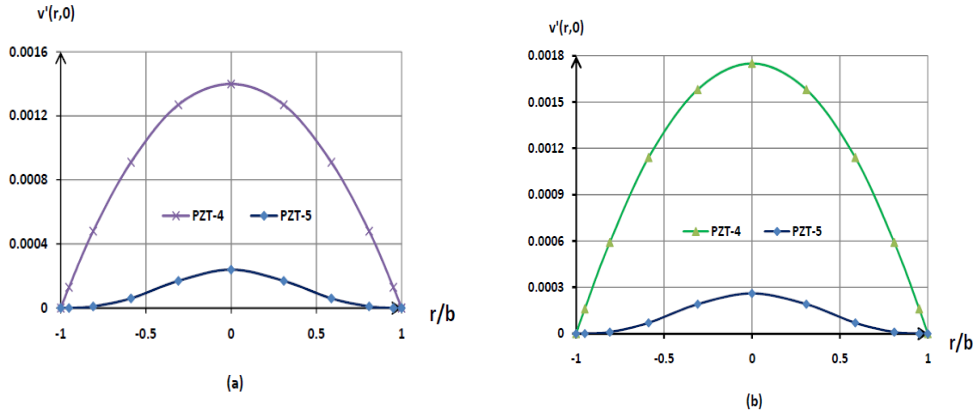

Fig.7(a) Comparison of normalized crack surface displacement $v'(r,0)$ for various ceramics in the case of compressive line load($Q = 0.50, \frac{a}{b} = 0.25, \frac{b}{h} = 0.75$) **(b)** Comparison of normalized crack surface displacement $v'(r,0)$ for various ceramics in the case of tensile line load ($Q = 0.20, a/b = 0.25, b/h = 0.75$).

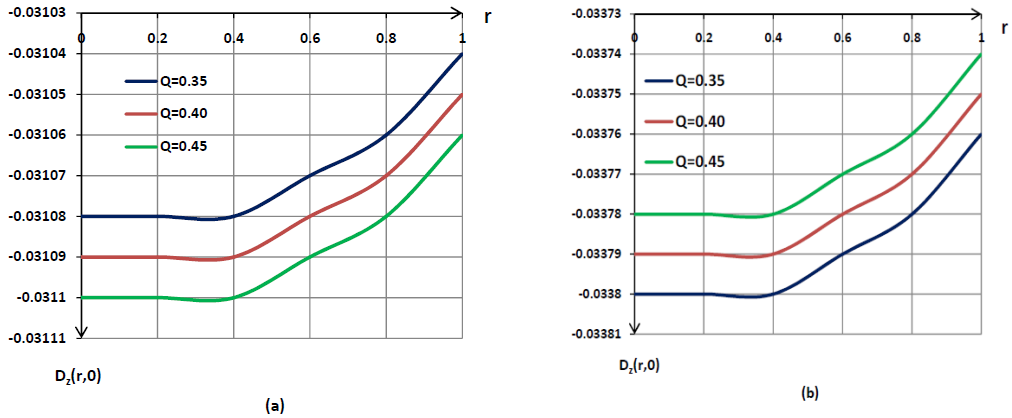

Fig.8 (a) Variation of electric displacement $Dz\,(r,0)$ with r for different values of Q for compressive line load $(a/b = 0.25, b/h = 0.75)$. **(b)** Variation of electric displacement $Dz\,(r,0)$ with r for different values of Q for tensile line load $(a/b = 0.25, b/h = 0.75)$.

Figs. 8(a,b) display variation of electric displacement $D_Z(r,0)$ with r, taking $\frac{a}{b} = 0.25, \frac{b}{h} = 0.75$ and different load ratio Q. Fig. 8(a) shows that electric displacement $D_Z(r,0)$ increases in magnitude with increasing Q in the case of compressive loading while the effect is just the opposite for tensile loadings (Fig.8(b)). The variation of $D_Z(r,0)$ with different $\frac{a}{b}$ and but fixed Q and $\frac{b}{h}$ are plotted in Figs 9(a, b). It is observed that for compressive loadings the electrical displacement numerically increases with the increase of $\frac{a}{b}$ values, while the effect is opposite in the case of tensile loadings.

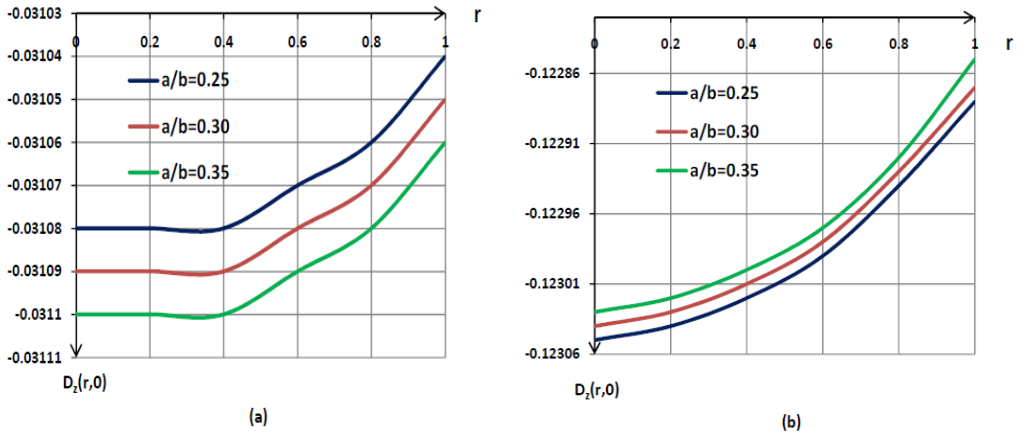

Fig.9 (a) Variation of electric displacement $D_Z(r,0)$ with r for different values of a/b for compressive line load $(Q = 0.35, b/h = 0.75)$. **(b)** Variation of electric displacement $D_Z(r,0)$ with r for different values of a/b for tensile line load $(Q = 0.50, b/h = 0.50)$.

6. Conclusion

The study investigates various aspects of the presence of a penny shaped crack located in the middle of a loaded anisotropic piezoelectric layer of finite thickness. It is observed that the applied line load can be suitably adjusted in controlling crack expansion. The position of the applied load, thickness of the layer with respect to the crack radius, piezoelectric and anisotropic properties, all are shown to have significant effects on every characteristic of a cracked medium.

References

1. Balu S., Kannan G.R., Rajalingam K., (2014) Static studies on piezoelectric/piezomagnetic composite structure under mechanical and thermal loading, *Int. J. Engg. Sci.& Research Technology*, Balu, February, 3(2), 678-685.
2. Barik S.P., Kanoria M,, Chaudhuri P.K., (2008) Effect of anisotropy on thermoelastic contact problem, *Appl. Math.Mech*., 29, 501-510.
3. Bhargava R.R., Verma P.R., (2013) Analysis of cracked piezo-electro-magnetic plate under mechanical, electric and magnetic small-scale-yielding, *Int. J. Appl. Math.Mech*., 9(20), 45-62.

4. Birinci A., Birinci F., Cakiroglu F.L., Erdol R., (2010) An internal crack problem for an infinite elastic layer, *Arch. Appl. Mech*., 80, 997-1005.
5. Chen W., Ding H., Hou P., (2001) Exact solution of an external circular crack in a piezoelectric solid subjected to shear loading, J. Zhejiang University (Science), 2(1), 9-14.
6. Dai M., Schiavone P., Gao C., (2016) An anisotropic piezoelectric half-plane containing an elliptical hole or crack subjected to uniform in-plane electromechanical loading, *J. Mech. Materials and Struc*., 11(4), DOI:10.2140/jomms.2016.11.433,433-448.
7. Dyka E., Rogowski B., (2005) On the contact problem for a smooth punch in piezoelectroelasticity, *J. Theo. Appl. Mech. Warsaw*, 43, 745-761.
8. Fabrikant V.I., (1996) Interaction of an arbitrary force with a flexible punch or with an external circular crack, *Int.J.Engg.Sci.*, 34, 1753-1765.
9. Gupta G.D., Erdogan F., (1974) The problem of edge cracks in an infinite strip, *J. Appl. Mech*., 41, 1001-1006.
10. Kalamkarov A.L., Pedro P.M.C.L., Savi M.A., Basu A., (2015) Analysis of Magneto-Piezoelastic Anisotropic Materials, *Metals*, 5, doi:10.3390/met5020863,863-880.
11. Karapetian E., Sevostianov I., Kachanov M., (2000) Penny-shaped and half-plane cracks in a transversely isotropic piezoelectric solid under arbitrary loading, *Arch. Appl. Mech.*, Springer-Verlag, 70, 201-229.
12. Ma C.C., Luo J.J., (1996) Plane solution of interface cracks in anisotropic dissimilar media, *J. Engg. Mech*., 122, 30-38.
13. Mishuris G.,Piccolroaz A.,Vellender A., (2014) Boundary integral formulation for cracks at imperfect interfaces, *Q. J. Mech. Appl. Math*.,67,363-387.
14. Nowacki W., Teoria Sprężystości, PWN, Warszawa, 1973.
15. Park S.B., Sun C.T., (1995) Fracture criteria for piezoelectric ceramics, *J. Am. Ceram. Soc.*, 78, 1475-1480.
16. Parton V.Z., Kudryatvsev B.A., Electromagnetoelasticity, Gordon and Breach, New York, 1988.
17. Patra R., Barik S.P., Kundu M., Chaudhuri P.K., (2014) Plane elastostatic solution in an infinite functionally graded layer weakened by a crack lying in the middle of the layer, *Int. J. Comp. Math*, Article ID 358617.
18. Patra R., Barik S.P., Chaudhuri P.K., (2015) An internal crack problem in an infinite transversely isotropic elastic layer, *Int. J. Adv. Appl. Math. and Mech*., 3(1), 62-70.
19. Rogowski B., (2009) Analysis of a penny-shaped crack in a magneto-elastic medium, *J. Theo. Appl. Mech*., 47(1), 143-159.
20. Singh B.M., Rokne J., Dhaliwal R.S., (2006) Closed-form solution for piezo-electric layer with two collinear cracks parallel to the boundaries, *Mathematical Problems in Engg*, Article ID 91846,116.
21. Wang B.L., Mai Y.W., (2002) A piezoelectric material strip with a crack perpendicular to its boundary surfaces, *Int. J. Solids and Struc*., 39, 4501-4524.
22. Wang M.Z.,Xu X., (1990) A generalization of Alamnsi's theorem and its application, *Appl. Math. Modelling*, 14, 275-279.
23. Wang Z., (1994) Penny-shaped crack in transversely isotropic piezoelectric materials, *Acta Mechanica Sinica*, 10(1), 49-60.
24. Xing L., Yongyi L., Pengpeng S., (2013) The thermal effect of anti-plane crack in a functionally graded piezoelectric strip under electric shock, 13th International Conference on Fracture, June 16-21, Beijing, China.